HENS Unchained: MILP Implementation of Multi-Stage Utilities with Stream Splits, Variable Temperatures and Flow Capacities

David Huber *, Felix Birkelbach and René Hofmann

Institute of Energy Systems and Thermodynamics, TU Wien, Getreidemarkt 9/E302, 1060 Vienna, Austria
* Correspondence: david.huber@tuwien.ac.at

Abstract: In this paper, we present an extended heat exchanger synthesis superstructure (HENS) formulation to consider streams with variable temperatures and flow capacities using mixed-integer linear programming (MILP). To keep the problem tractable and to leverage the potential of state-of-the-art MILP solvers, piecewise-linear models with logarithmic coding are used. Allowing for variable utility parameters within a feasible technical range, instead of a priori defined ones, removes limitations of the HENS. Increasing the utility's degree of freedom offers advantages when sensible heat from, for example, flue gas, thermal oil, or water is used. Moreover, utilities are no longer limited to single-stage heat transfer without stream splits at the stream ends, generating opportunities for efficiency enhancement. We consider three representative case studies to evaluate the performance of the unchained HENS method. Our results show that representing utilities as streams in the HENS optimization problem leads to lower total annual costs (TAC). Significant cost savings arise due to more efficient utility placement, heat transfer, and smaller heat exchanger areas. The results indicate that this method can lead to cheaper and more resource-efficient HEN and thus positively contribute to the environment.

Keywords: heat exchanger network synthesis; multi-stage utilities with stream splits; intermediate utility placement; piecewise-linear approximation; mixed-integer linear programming

1. Introduction

Agreed climate targets can only be met through a radical reduction in greenhouse gas emissions. Energy-intensive industries are responsible for a significant share of these emissions. The economic pressure of reducing emissions requires companies to pursue cost-effective solutions. One way to reduce emissions cost-effectively is to connect hot and cold process streams. A heat exchanger network (HEN) enables heat exchange between process streams and thus reduces the energy demand for heating or cooling. The design of an HEN is a complex task due to the high combinatorics of numerous possible connections between streams. Based on the objective function, an optimal HEN can be determined by applying heat exchanger network synthesis (HENS).

The HEN design problem was first mentioned by Ten Broeck in 1944 [1]. The first formal definition was published by Masso and Rudd in 1969 [2]. All these approaches are sequential methods that decompose the HENS problem into a set of subproblems. Decomposition requires parameter estimation and iterative optimization, which is why the optimal solution is challenging to find. Fully simultaneous methods calculate the optimal utility consumption, stream matches and HEN configuration simultaneously [3]. The first simultaneous HENS were published by Yuan et al. [4] in 1989, Yee and Grossmann [5] in 1990 and Ciric and Floudas [3] in 1991. For a more detailed elaboration of the historical development, the papers by Furman and Nikolaos [6] and Escobar and Trierweiler [7] are recommended. The latter have shown in their work that Yee and Grossmann's stage-wise superstructure formulation [5] gives better results in terms of total annual cost (TAC) at lower computation times. Therefore,

in this paper, we will build on this formulation. Further interesting approaches can be found in the work of Gu et al. [8] and Zirngast et al. [9]. In contrast to the traditional methods, the latter two address uncertainties in the stream definition.

In Yee and Grossmann's formulation, two assumptions are made that may lead to sub-optimal HENs: First, implementing utilities is only possible with predefined inlet and outlet temperatures. This assumption is only reasonable where utilities condense a medium at a constant temperature and pressure. If only the sensitive heat in, for example, flue gas or cooling water is used, the temperatures to which the medium must be cooled or heated are of minor importance. Usually, there is a margin for utility temperatures in terms of regulatory and process requirements. Secondly, the utilities must always reach the set temperature in only one heat exchanger without stream splits. In contrast, hot and cold process streams can reach their set target temperature using multi-staged heat exchangers with stream splits. These two limitations inhibit the field application. Considering multi-stage utilities with variable temperatures is essential to optimally integrate the heat sink and source into the process. To run HENS without these assumptions, the Yee and Grossmann formulation has to be adapted.

Yee and Grossmann's non-linear formulation belongs to the class of $\mathcal{NP}$-hard problems [10]. Even with state-of-the-art computational power and solvers, the optimal heat integration of complex industrial processes cannot be calculated. Implementing utilities as streams with variable temperatures and flow capacities further increases the complexity of the optimization problem. Martelli et al. [11], for example, proposed an MINLP model for complex utility handling using a two-stage algorithm. Moreover, it can never be guaranteed that the optimal solution has been found. Piecewise-linear approximation of the non-linear terms (mean logarithmic temperature difference (LMTD), heat exchanger areas, and energy balances) is necessary to find a global minimum within feasible computation time, even though the problem is still $\mathcal{NP}$-hard. Beck and Hofmann [12] linearized the superstructure formulation and applied mixed-integer linear programming (MILP) to solve the problem. Compared to the non-linear model, they achieved better results in terms of TAC with shorter computation times.

Paper Organization

This paper presents a novel piecewise-linear implementation of utilities as multi-stage streams with stream splits, variable temperatures, and flow capacities. The methods in Section 2 are divided into two main sections. First, all our essential adaptations of the superstructure formulation are presented in Section 2.1. In Section 2.2, the piecewise-linear approximation of the non-linear terms with hyperplanes and simplices and the transfer to MILP is shown. Section 3 introduces three representative use cases from the literature and industrial problems. For each use case, either a cold utility or a cold and a hot utility is implemented as a stream with variable outlet temperature and heat capacity flow. A comparison is made for the results with and without variable utility definitions. We show that minor variations in the utility outlet temperature lead to a significant improvement in terms of TAC. We therefore conclude in Section 4 that variable outlet temperatures and flow capacities allow the cost-optimal design of the necessary utilities.

2. Methods

2.1. Modification of the Superstructure

One way of realizing multi-stage utilities is to implement them as streams with stream splits. However, one consequence is that the flow capacity must be specified. If one degree of freedom is blocked by setting the flow capacity for the utility stream, the utilities may not necessarily provide the required energy for heating or cooling the streams. Introducing an additional variable for the flow capacity makes the optimization problem non-linear again. Implementing a variable outlet temperature requires another variable. Both variables are independent and form non-linear relationships, further increasing the complexity of the problem.

Referring to the stage-wise superstructure according to Yee and Grossmann [5], cold (UC) and hot utilities (UH) can only be located at the end of the streams. The streams can exchange heat in N_{st} stages.

In this paper, we extend the formulation to implement hot and cold utilities as streams—hereafter referred to as utility streams (US). The objective function

$$\min TAC =$$

$$\underbrace{\sum_i c_{\text{cu}}\, q_{\text{cu},i} + \sum_i \sum_{j \in CP} \sum_k c_{\text{cu}}\, q_{ijk}}_{\text{cold utility costs}} + \underbrace{\sum_j c_{\text{hu}}\, q_{\text{hu},j} + \sum_{i \in HP} \sum_j \sum_k c_{\text{hu}}\, q_{ijk}}_{\text{hot utility costs}}$$

$$+ \underbrace{\sum_i \sum_j \sum_k c_{\text{f}}\, z_{ijk} + \sum_i c_{\text{f}}\, z_{\text{cu},i} + \sum_j c_{\text{f}}\, z_{\text{hu},j}}_{\text{step-fixed investment costs}}$$

$$+ \underbrace{\sum_i \sum_j \sum_k c_{\text{v}} \left(\frac{q_{ijk}}{U_{ij}\, LMTD_{ijk}} \right)^{\beta}}_{\text{variable HEX stream costs}}$$

$$+ \underbrace{\sum_i c_{\text{v}} \left(\frac{q_{\text{cu},i}}{U_{\text{cu},i}\, LMTD_{\text{cu},i}} \right)^{\beta}}_{\text{variable HEX cold utility costs}} + \underbrace{\sum_j c_{\text{v}} \left(\frac{q_{\text{hu},j}}{U_{\text{hu},j}\, LMTD_{\text{hu},j}} \right)^{\beta}}_{\text{variable HEX hot utility costs}} \tag{1}$$

where

$$U_{ij} = \left(\frac{1}{h_i} + \frac{1}{h_j} \right)^{-1} \quad : \quad i \in HP,\ j \in CP$$

$$U_{\text{cu},i} = \left(\frac{1}{h_{\text{cu}}} + \frac{1}{h_i} \right)^{-1} \quad : \quad i \in HP \tag{2}$$

$$U_{\text{hu},j} = \left(\frac{1}{h_{\text{hu}}} + \frac{1}{h_j} \right)^{-1} \quad : \quad j \in CP$$

and

$$LMTD_{ijk} = \frac{\Delta T_{i,j,k} - \Delta T_{i,j,k+1}}{\ln \frac{\Delta T_{i,j,k}}{\Delta T_{i,j,k+1}}} \quad : \quad i \in HP,\ j \in CP,\ k \in ST$$

$$LMTD_{\text{cu},i} = \frac{\Delta T_{\text{cu1},i} - \Delta T_{\text{cu2},i}}{\ln \frac{\Delta T_{\text{cu1},i}}{\Delta T_{\text{cu2},i}}} \quad : \quad i \in HP \tag{3}$$

$$LMTD_{\text{hu},j} = \frac{\Delta T_{\text{hu1},j} - \Delta T_{\text{hu2},j}}{\ln \frac{\Delta T_{\text{hu1},j}}{\Delta T_{\text{hu2},j}}} \quad : \quad j \in CP$$

minimizes the TAC of the heat exchanger network.

If the flow capacity and the outlet temperature are constant, Equation (4) is used to constrain the utility heat loads.

$$q_{\text{cu},i} = F_i \left(T_{i,k=N_{\text{st}}+1} - T_{i,k=N_{\text{st}}+2} \right) \quad : \quad i \in HP \backslash (H_{\text{F}} \cap H_{\text{Tout}})$$

$$q_{\text{hu},j} = F_j \left(T_{j,k=1} - T_{j,k=2} \right) \quad : \quad j \in CP \backslash (C_{\text{F}} \cap C_{\text{Tout}}) \tag{4}$$

If hot utility streams (HUS) and/or cold utility streams (CUS) are implemented, the utilities are no longer necessary and disabled with Equation (5).

$$
\begin{aligned}
z_{\text{cu},i} = 0 \quad &: \quad i \in H_{\text{F}} \\
z_{\text{hu},j} = 0 \quad &: \quad j \in C_{\text{F}}
\end{aligned}
\tag{5}
$$

The heat exchange between utilities and streams always occurs at the stream ends in only one stage and without stream splits. This results in a total of $N_{\text{st}} + 1$ stages for heat exchange with other streams and the utility. Due to the disabled utilities, only N_{st} stages are available for the US heat exchange. Increasing the number of stages by one ensures that the same number of stages are available for heat exchange compared to the original superstructure formulation.

$$
\begin{aligned}
z_{i,j,k=1} = 0 \quad &: \quad i \in HP \backslash H_{\text{F}}, \ j \in CP \\
z_{i,j,k=N_{\text{st}}+1} = 0 \quad &: \quad j \in CP \backslash C_{\text{F}}, \ i \in HP
\end{aligned}
\tag{6}
$$

Blocking the stream heat exchange with Equation (6) at the added stage secures the stream-to-stream heat exchange at the initial $N_{\text{st}} + 1$ stages.

The temperatures at position $k = 1$ and $k = N_{\text{st}} + 2$ in Equations (7) and (8) correspond to the inlet and outlet temperatures of the streams.

$$
\sum_j \sum_k q_{ijk} + q_{\text{cu},i} = F_i \left(T_{i,k=1} - T_{i,k=N_{\text{st}}+2} \right) \quad : \quad i \in HP
\tag{7}
$$

$$
\sum_i \sum_k q_{ijk} + q_{\text{hu},j} = F_j \left(T_{j,k=1} - T_{j,k=N_{\text{st}}+2} \right) \quad : \quad j \in CP
\tag{8}
$$

If at least two of the three variables on the right side are assigned a discrete value with Equations (11), (13) or (14), the constraints of the stream-wise energy balance remain linear. If fewer values are set, the piecewise-linear approximation presented in Section 2.2.3 is used.

The stage-wise energy balance can be constrained with Equation (9). If the flow capacity F_i is not set to a predefined value with Equation (11), the piecewise-linear approximation from Section 2.2.3 is used.

$$
\sum_j q_{ijk} = F_i \left(T_{i,k} - T_{i,k+1} \right) \quad : \quad i \in HP, \ k \in ST
\tag{9}
$$

$$
\sum_i q_{ijk} = F_j \left(T_{j,k} - T_{j,k+1} \right) \quad : \quad j \in CP, \ k \in ST
\tag{10}
$$

The flow capacities are set to a specific value with Equation (11). Otherwise, F is bounded to the predefined range $[F_{\text{min}}^{\text{set}}, F_{\text{max}}^{\text{set}}]$ with Equation (12).

$$
\begin{aligned}
F_i = F_i^{\text{set}} \quad &: \quad i \in HP \backslash H_{\text{F}} \\
F_j = F_j^{\text{set}} \quad &: \quad j \in CP \backslash C_{\text{F}}
\end{aligned}
\tag{11}
$$

$$
\begin{aligned}
F_{i,\text{min}}^{\text{set}} \leq F_i \leq F_{i,\text{max}}^{\text{set}} \quad &: \quad i \in H_{\text{F}} \\
F_{j,\text{min}}^{\text{set}} \leq F_j \leq F_{j,\text{max}}^{\text{set}} \quad &: \quad j \in C_{\text{F}}
\end{aligned}
\tag{12}
$$

Constant inlet or outlet temperatures are set with Equations (13) and (14). Variable temperatures are constrained to a specified range for the inlet temperature $[T_{\text{min}}^{\text{in}}, T_{\text{max}}^{\text{in}}]$ and the range for the outlet temperature $[T_{\text{min}}^{\text{out}}, T_{\text{max}}^{\text{out}}]$ using Equations (15) and (16), respectively.

$$
\begin{aligned}
T_{i,k=1} = T_i^{\text{in}} \quad &: \quad i \in HP \backslash H_{\text{Tin}} \\
T_{j,k=N_{\text{st}}+2} = T_j^{\text{in}} \quad &: \quad j \in CP \backslash C_{\text{Tin}}
\end{aligned}
\tag{13}
$$

$$T_{i,k=N_{st}+2} = T_i^{out} \quad : \quad i \in HP \backslash H_{Tout}$$
$$T_{j,k=1} = T_j^{out} \quad : \quad j \in CP \backslash C_{Tout} \tag{14}$$

$$T_{i,min}^{in} \leq T_{i,k=1} \leq T_{i,max}^{in} \quad : \quad i \in H_{Tin}$$
$$T_{j,min}^{in} \leq T_{j,k=N_{st}+2} \leq T_{j,max}^{in} \quad : \quad j \in C_{Tin} \tag{15}$$

$$T_{i,min}^{out} \leq T_{i,k=N_{st}+2} \leq T_{i,max}^{out} \quad : \quad i \in H_{Tout}$$
$$T_{j,min}^{out} \leq T_{j,k=1} \leq T_{j,max}^{out} \quad : \quad j \in C_{Tout} \tag{16}$$

Note that, if stream inlet and outlet temperatures are defined in a specific range, the conditions

$$T_{i,min}^{in} \geq T_{i,max}^{out} \quad : \quad i \in H_{Tin} \cap H_{Tout}$$
$$T_{j,max}^{in} \leq T_{j,min}^{out} \quad : \quad j \in C_{Tin} \cap C_{Tout} \tag{17}$$

must always be fulfilled to obtain a feasible solution.

The following constraints are not affected by variable temperatures or flow capacities. Monotonic decrease in temperature:

$$T_{i,k} \geq T_{i,k+1} \quad : \quad i \in HP, k \in ST$$
$$T_{j,k} \geq T_{j,k+1} \quad : \quad j \in CP, k \in ST \tag{18}$$

Bounds for heat loads:

$$z_{i,j,k}\,\omega_s \leq q_{i,j,k} \leq z_{i,j,k}\,\Omega_s \quad : \quad i \in HP, j \in CP, k \in ST$$
$$z_{cu,i}\,\omega_{cu} \leq q_{cu,i} \leq z_{cu,i}\,\Omega_{cu} \quad : \quad i \in HP$$
$$z_{hu,j}\,\omega_{hu} \leq q_{hu,j} \leq z_{hu,j}\,\Omega_{hu} \quad : \quad j \in CP \tag{19}$$

Bounds for temperature differences:

$$\Delta T_{min} \leq \Delta T_{i,j,k}$$
$$\Delta T_{i,j,k} \leq T_{i,k} - T_{j,k} + \Gamma\left(1 - z_{i,j,k}\right) \, : \, i \in HP, j \in CP, k \in ST$$
$$\Delta T_{i,j,k+1} \leq T_{i,k+1} - T_{j,k+1} + \Gamma\left(1 - z_{i,j,k}\right) \tag{20}$$

$$\Delta T_{min} \leq \Delta T_{cu1,i} \leq T_{i,k=N_{st}+1} - T_{cu}^{out} + \Gamma(1 - z_{cu,i})$$
$$\Delta T_{min} \leq \Delta T_{cu2,i} \leq T_{i,k=N_{st}+2} - T_{cu}^{in} + \Gamma(1 - z_{cu,i}) \quad : \quad i \in HP \tag{21}$$

$$\Delta T_{min} \leq \Delta T_{hu1,j} \leq T_{hu}^{out} - T_{j,k=2} + \Gamma(1 - z_{hu,j})$$
$$\Delta T_{min} \leq \Delta T_{hu2,j} \leq T_{hu}^{in} - T_{j,k=1} + \Gamma(1 - z_{cu,j}) \quad : \quad j \in CP \tag{22}$$

Integrality:

$$z_{i,j,k},\ z_{cu,i},\ z_{hu,j} \quad : \quad i,j,k \in \{0,1\} \tag{23}$$

Non-negativity constraints:

$$q_{i,j,k},\ q_{cu,i},\ q_{hu,j} \geq 0 \quad : \quad i \in HP, j \in CP, k \in ST \tag{24}$$

2.2. Piecewise-Linear Approximation

To integrate the design of the utilities into the HENS and find a global optimum within a feasible computation time, piecewise-linear approximation is essential. For the sake of simplicity, a function with one primary curvature is called convex or concave accordingly. In contrast to the convex heat exchanger area of the streams and the concave heat exchanger surface of the utilities, the energy balance is neither convex nor concave. The energy balance is essentially a multiplication of two independent variables. The resulting saddle-shaped function can no longer be represented with sufficient accuracy by simple concave or convex approximations. Therefore, the following two methods for linear approximation are distinguished in this paper: Piecewise-linear approximation with hyperplanes and with simplices. Piecewise-linear approximation with hyperplanes is used for the convex function of the stream HEX area (see Section 2.2.1) and the concave function of the utility HEX area (see Section 2.2.2). Each hyperplane is defined linear function with coefficients *a*, which specifies offset and slope. The coefficients *a* are determined using a nonlinear optimization that minimizes the sum of squares error (SSE) between the linearized planes and the data points. Concave functions can be linearized in the same way by considering the identity $\min(y) = -\max(-y)$. The accuracy of the approximation can be adjusted by adding hyperplanes until a defined root-mean-square error (RMSE) is reached. In contrast to piecewise-linear approximation with simplices, only limited accuracy can be achieved for non-convex or non-concave approximations.

Convex or concave approximation with hyperplanes is only suitable for functions that curve in only one direction. In the natural sciences, however, problems often occur which require a multiplication of optimization variables. For example, the two-dimensional function $f(y) = x_1 x_2$ is saddle-shaped and cannot be approximated convexly or concavely with sufficient accuracy. By contrast, any continuous function can be approximated piecewise-linearly with simplices. In the two-dimensional set, for a grid with w elements, the function $f : [0, w]^2 \to \mathbb{R}$ can be divided into triangles [13]. The function f can thus be approximated with piecewise functions linearly within the triangles. In this paper, the J_1 union jack triangulation is used. This method requires a grid with the nodes of the triangles in its intersection. A non-linear optimization problem determines the grid points and the plane equations of the triangles by minimizing the SSE. Piecewise-linear approximation with simplices is used for the stream- and stage-wise energy balances (see Section 2.2.3) and the LMTD (see Section 2.2.4).

2.2.1. Stream Heat Exchanger Area

The reduced heat exchanger area

$$\tilde{A}_{ijk} = \left(\frac{q_{ijk}}{U_{ij} \, LMTD_{ijk}} \right)^{\beta} \tag{25}$$

for a stream HEX is a convex function. Beck et al. formulate a linear optimization problem to constrain the independent variables q and *LMTD* to a physically feasible domain. The N_{hyp} hyperplanes of the two-dimensional function are defined with coefficients *a* such that $\tilde{A} = a_0 + a_1 \, \text{LMTD} + a_2 \, q$ for each data point. Figure 1 shows the reduced solution space with 2014 data points in a light gray and hyperplane approximation for two example streams. Within this example, we are able to achieve an RMSE of 1.26% using 5 hyperplanes. Above 22 hyperplanes, the RMSE of 1.16% does not change within the lsqnonlin solver's step size tolerance of 10^{-6}.
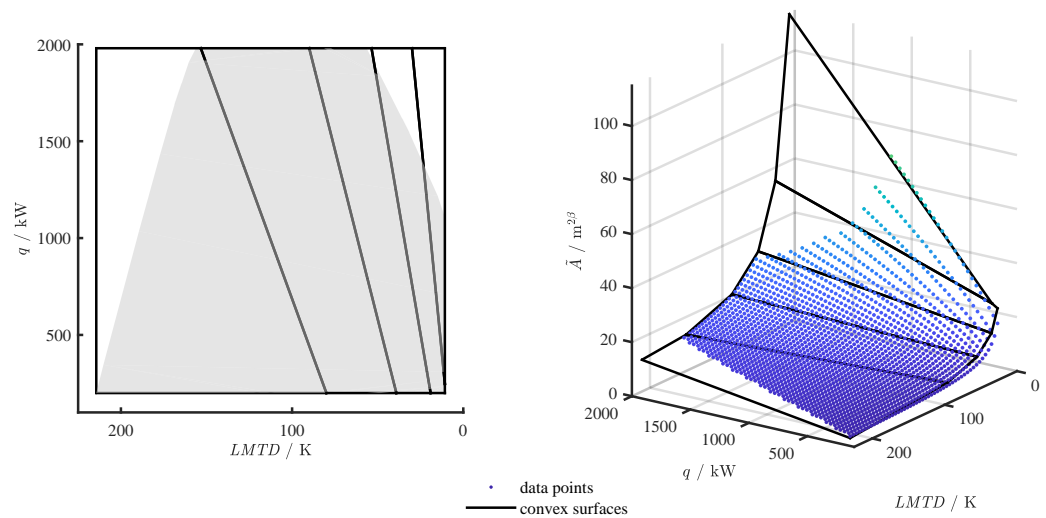
Figure 1. Piecewise-linear approximation of the reduced stream HEX area $\tilde{A}$ as a function of the heat flow q and *LMTD* with five hyperplanes. Hot stream: $T^{\text{in}} = 270\,^\circ\text{C}$, $T^{\text{out}} = 160\,^\circ\text{C}$, $F = 18\,\text{kW/K}$, $h = 1\,\text{kW/(m}^2\,\text{K)}$. Cold stream: $T^{\text{in}} = 50\,^\circ\text{C}$, $T^{\text{out}} = 210\,^\circ\text{C}$, $F = 20\,\text{kW/K}$, $h = 1\,\text{kW/(m}^2\,\text{K)}$. $\beta = 0.8$. *RMSE* $= 1.26\%$.

2.2.2. Utility Heat Exchanger Area

Since three out of four temperatures are fixed at the utility heat exchangers, the reduced heat exchanger area can be formulated as a function of the heat flow q [12]. The one-dimensional correlation of the reduced heat exchanger area for hot utilities

$$
\tilde{A}_{\text{hu},j}(q_{\text{hu},j}) = \left[\frac{q_{\text{hu},j}\left(\ln\left(T_{\text{hu}}^{\text{in}} - T_j^{\text{out}}\right) - \ln\left(T_{\text{hu}}^{\text{out}} - T_j^{\text{out}} + \frac{q_{\text{hu},j}}{F_j}\right)\right)}{U_{\text{hu},j}\left(T_{\text{hu}}^{\text{in}} - T_{\text{hu}}^{\text{out}} + \frac{q_{\text{hu},j}}{F_j}\right)} \right]^{\beta}
\tag{26}
$$

and cold utilities

$$
\tilde{A}_{\text{cu},i}(q_{\text{cu},i}) = \left[\frac{q_{\text{cu},i}\left(\ln\left(T_i^{\text{out}} + \frac{q_{\text{cu},i}}{F_i} - T_{\text{cu}}^{\text{out}}\right) - \ln\left(T_i^{\text{out}} - T_{\text{cu}}^{\text{in}}\right)\right)}{U_{\text{cu},i}\left(\frac{q_{\text{cu},i}}{F_i} - T_{\text{cu}}^{\text{out}} + T_{\text{cu}}^{\text{in}}\right)} \right]^{\beta}
\tag{27}
$$

is a concave function. Equations (26) and (27) are restricted to the physically solvable domain and represented by lines. The lines are thus represented as linear equations $\tilde{A} = a_0 + a_1\,q$ for each plane and heat exchanger. The coefficients are determined by non-linear minimization of the SSE until an RMSE criterion is met. Figure 2 shows the concave function of the reduced utility HEX area with 25 data points and the piecewise-linear approximation. With four lines, an RMSE of 0.38% can be achieved. In this case, an ideal linear approximation would be possible by interpolating the data points. In this case, the improved accuracy is out of proportion to the required binary variables, which unnecessarily increases the complexity and computation time of the optimization problem.
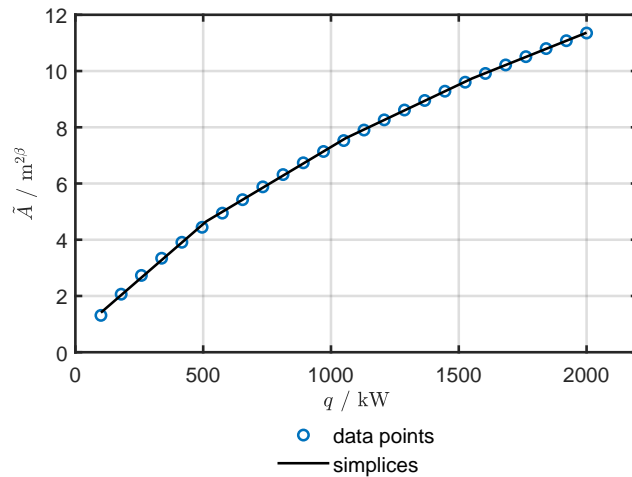
Figure 2. Piecewise-linear approximation of the reduced utility HEX area $\tilde{A}$ as a function of the heat flow q with four lines. Hot stream: $T^{\text{in}} = 270\,°\text{C}$, $T^{\text{out}} = 160\,°\text{C}$, $F = 18\,\text{kW/K}$, $h = 1\,\text{kW/(m}^2\,\text{K)}$. Cold utility: $T^{\text{in}} = 10\,°\text{C}$, $T^{\text{out}} = 30\,°\text{C}$, $h = 1\,\text{kW/(m}^2\,\text{K)}$. $\beta = 0.8$. *RMSE* $= 0.38\%$.

2.2.3. Energy Balances

The piecewise-linear approximation of the energy balances, Equations (7)–(10), is of central importance to implementing streams with variable inlet or outlet temperature and flow capacity. Figure 3 shows the 900 data points and the piecewise-linear approximation with simplices of a streamwise-energy balance. The heat flow q is plotted as a function of the flow capacity F and the temperature difference $T^{\text{in}} - T^{\text{out}}$. The saddle-shaped function is approximated with 32 simplices on an equidistant 4×4 grid with an RMSE of 0.28%.
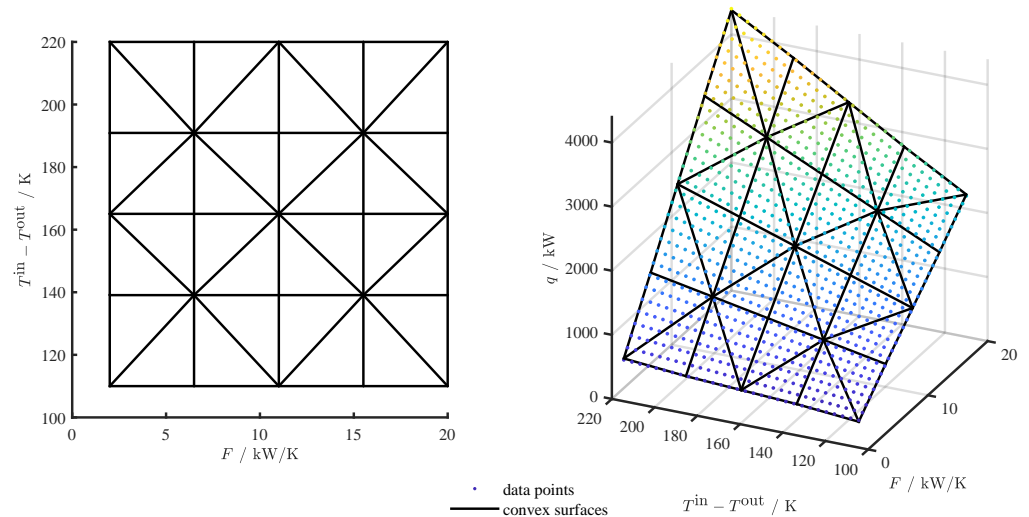

Figure 3. Piecewise-linear approximation of the stream-wise energy balance as a function of the flow capacity F and the temperature difference $T^{\text{in}} - T^{\text{out}}$ with 32 simplices. Hot stream: $T^{\text{in}} = 270\,°\text{C}$, $T^{\text{out}} = [50, 160]\,°\text{C}$, $F = [2, 20]\,\text{kW/K}$. *RMSE* $= 0.28\%$.

2.2.4. LMTD

The LMTD, according to Equation (3), is concave and can be approximated with hyperplanes and simplices. Both methods require additional binary variables. The approximation with simplices offers considerable advantages in terms of the MILP translation. Significantly higher accuracies can be achieved with the same number of binary variables. Figure 4 shows the piecewise-linear approximated LMTD with 900 data points on a 4×4 grid. In regions with larger curvature, more simplices are placed.
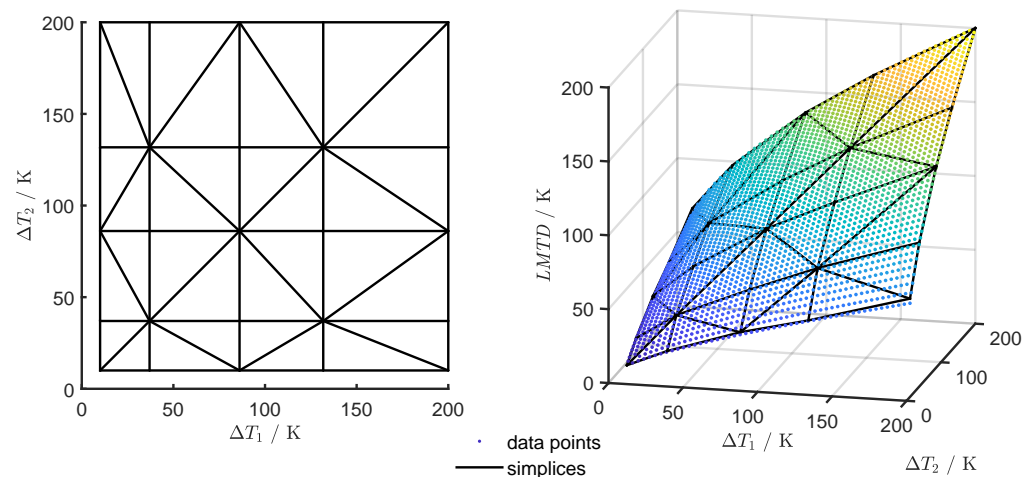
Figure 4. Piecewise-linear approximation of the *LMTD* as a function of the two temperature differences ΔT_1 and ΔT_2. *LMTD* in the range from $10\,\text{K}$ to $200\,\text{K}$. *RMSE* $= 0.34\%$.

2.3. Translation to MILP

The translation to MILP should be carried out with as few auxiliary binary and continuous variables as possible. Thus, the minimization problem can be solved efficiently within a feasible timeframe.

The streams' convex reduced HEX area is translated most easily to MILP. The hyperplanes shown in Figure 1 can be translated to MILP with one inequality each and without additional binary variables, see [12].

For all other functions, binary variables are necessary to translate the simplices into MILP. Vielma and Nemhauser [13] developed a logarithmic approach to reduce the number of binary variables. A grid with w elements in an n-dimensional space, where w is a power of two, is composed of $T = w^n\, n!$ simplices. The T simplices can be translated to MILP highly efficiently with $n \log_2 w + {}^{n(n-1)}/_2$ binary variables and $(w+1)^n$ continuous variables. The piecewise-linear approximations based on simplices presented in the previous sections are all on a grid with $w = 4$ elements in each dimension. The one-dimensional approximation of the utility HEX area in Figure 2 is modeled with four simplices. Thus, two binary variables and four additional constraints are used to translate the correlation to MILP. On the other hand, the widely used SOS2 approach would require four binary variables. The approximation of the two-dimensional correlations for the streams HEX area, energy balance, and LMTD is composed of 32 simplices. These can be translated to MILP with five binary variables and ten additional constraints each. Due to the small number of binary variables combined with the high accuracy of the approximation, non-linear correlations can be approximated highly efficiently and modern MILP solvers can calculate a global optimum in feasible computing time.

Since not all approximations reach the value $f(0) = 0$, the functions are toggled with binary variables and a big-M approach. The hyperplane approximation's maximum value always occurs in the corner of the domain. Accordingly, the big-M value is chosen. By choosing the smallest possible big-M value, the problem remains tight and the stability of the numerical solving algorithms is improved because the feasible region of the LP relaxation is not unnecessarily expanded [14].

3. Case Studies & Results

This paper examines whether it is beneficial in terms of TAC to implement utilities as multi-stage streams with stream splits and variable outlet temperature and flow capacity. Furthermore, the influence of the utility outlet temperature on the TAC is studied. For this purpose, in each of the three representative case studies (CS), all utilities that only use sensible heat are implemented as streams. To ensure comparability with the results from the literature, we use only cost factors proportional to the utility heat flow.

Depending on the utilities, the following cases were considered:

base For each case study, the base case is used to compare the results with literature values and to validate the optimization framework.

var UC A cold utility with variable outlet temperature and flow capacity is implemented when only the sensible heat of a medium such as water or thermal oil is used for cooling.

var UC & UH A hot and cold utility with variable outlet temperature and flow capacity is implemented when only the sensible heat is used for both cooling and heating.

3.1. Piecwise-Linear Approximation & Implementation

Planes were added to the linear models of the stream HEX area until the RMSE was below 1.0%. To limit the number of binaries used to transfer the simplices to MILP, the approximation of the utility HEX area, energy balances, and LMTD were calculated on a 4×4 grid with 32 simplices. The *RMSE* is below 0.5 % for all models.

All optimization problems in this paper were modeled using Yalmip R20210331 [15] in Matlab R2022b [16]. All problems were solved using Gurobi 9.5.2 on a 128-core system (AMD EPYC 7702P) with 256 GB of RAM.

Each optimization problem was solved three times. The solution with the lowest computation time is presented. The convergence behavior over time is shown in Appendix A with its characteristic values, relative gap, upper and lower objective bounds. The relative gap is defined as the gap between the best feasible solution objective and the best bound. The calculations are terminated if the relative gap is smaller or equal than the tolerance of the MIP solver. The default value is 0.01%.

3.2. Case Study 1

The first case study was presented by Ahmad [17] and is composed of two hot and two cold streams. The stream data is listed in Table 1. Since the latent heat of steam is used as the hot utility, the outlet temperature of the steam cannot be adjusted without changing the steam parameters. Accordingly, no HUS is implemented. Since only the sensible heat of the cooling water is used, the cold utility is implemented as CUS. The CUS stream definition is marked with the superscript v. The parentheses specify the range of permissible values for the outlet temperature and the flow capacity.

Table 1. Stream data for case study 1: Ahmad [17].

Stream	T^{in} / °C	T^{out} / °C	F / kW/K	h / kW/m^2/K
H1	260	160	3.0	0.4
H2	250	130	1.5	0.4
C1	120	235	2.0	0.4
C2	180	240	4.0	0.4
UH	280	279	-	0.4
UC	30	80	-	0.4
UC^v	30	$[31, 80]$	$(0, 20)$	0.4

HEX costs: $c_f = 0\,\$/y$, $c_v = 300\,\$/(m^{2\beta}\,y)$, $\beta = 0.5$; Utility costs: $c_{hu} = 110\,\$/(kW\,y)$, $c_{cu} = 12.2\,\$/(kW\,y)$; Min. approach temperature: $\Delta T_{min} = 1\,°C$.

Results

The number of variables, the computation time, and the relative gap for CS1 can be seen in Table 2. The number of binary variables increases significantly with one implemented CUS from 120 to 376. Therefore, the computation time for the var UC case of 22.79 s is nearly ten times that of the base case with 2.30 s.

Table 2. Problem size, computation time and relative gap for CS1.

| Case	Variables / -	Binaries / -	Time / s	Rel. Gap / %
base	321	120	2.30	0.0000
var UC	3610	376	22.79	0.0009

To validate the developed framework, the base case is compared with three references from the literature. The results are summarized in Table 3. The stream plots of the resulting HENs are shown in Appendix B. The optimal HENs of Ahmad [17], Nielsen et al. [18], and Khorasany and Fesanghary [19] were calculated without using stream splits. Khorasany and Fesanghary [19] used a two-level approach with a harmony search algorithm and sequential quadratic programming to determine the best known literature value for minimum TAC of 1.1895×10^4 \$/y. In contrast to the literature values, we used three stages instead of four and allowed for stream splits.

We were able to find a solution for the base case with 1.1792×10^4 \$/y of TAC. In terms of TAC, the calculated solution is 0.87 % cheaper than the best literature value from Khorasany and Fesanghary [19]. Since both the values of the TAC and the heat loads show only minor deviations, it can be assumed that the framework presented in this paper provides reliable results.

Table 3. Results for CS1: Comparison of costs and heat loads at the utilities and streams.

Reference	TAC / 10^4 \$/y	Heat Load / kW		
		CU	HU	Stream
Ahmad [17]	1.2870	60.00	50.00	420.00
Nielsen et al. [18]	1.2306	45.00	36.00	434.00
Khorasany & Fesanghary [19]	1.1895	28.10	18.10	451.91
this work—base	1.1792	25.52	15.52	454.48
this work—var UC	1.1767	25.59	15.59	454.41

Implementing the CUS, we can find a solution with 1.08% lower TAC than the best literature value provided by Khorasany and Fesanghary [19]. Compared to the base case, 0.29% can be saved. As seen from the cost structure in Figure 5, the energy costs of the hot and cold utilities slightly increase compared to the base case. The main cost-saving results from the smaller heat exchanger area at the cold utility. The stream matches of the two resulting HENs are both identical; see Appendix B. Accordingly, the heat exchanger costs of the streams are almost identical. The outlet temperature of the CUS of 31.5 °C is close to the lower valid range of 31 °C. In contrast to the CU of the base case, the CUS temperature difference between the inlet and the outlet is reduced from 15 K to 1.5 K. The reduced temperature difference results in a large LMTD, which in turn results in a smaller and less expensive HEX area.
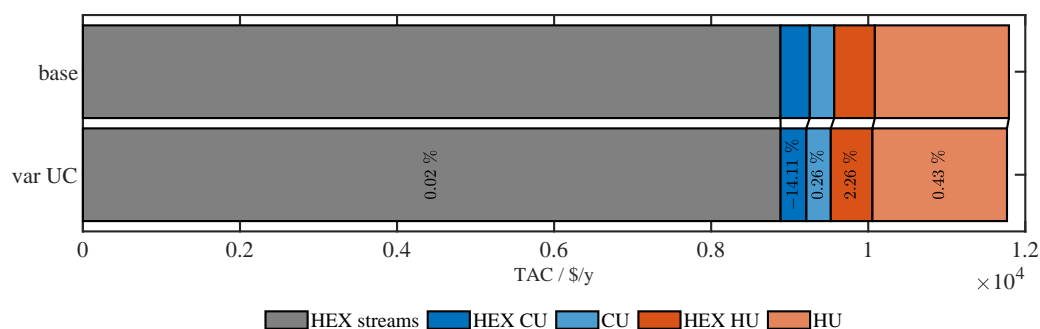
Figure 5. Breakdown of the cost structure for CS1. Relative cost savings in relation to the cost components of the base case.

3.3. Case Study 2

In the second case study, a frequently discussed aromatics plant in the literature is considered. The stream data provided by Linnhoff and Ahmad [20] is given in Table 4. In this case study, thermal oil is used as hot utility. Since only the sensible heat of the oil is used, the outlet temperature can be adjusted and the hot utility is implemented as HUS. The cold utility uses the sensible heat of cooling water and is therefore implemented as CUS. In contrast to CS1, two streams with variable outlet temperatures and flow capacities are implemented.

Table 4. Stream data for case study 2: Linnhoff & Ahmad [20].

Stream	T^{in} / °C	T^{out} / °C	F / kW/K	h / kW/m²/K
H1	327	40	100	0.50
H2	220	160	160	0.40
H3	220	60	60	0.14
H4	160	45	400	0.30
C1	100	300	100	0.35
C2	35	164	70	0.70
C3	85	138	350	0.50
C4	60	170	60	0.14
C5	140	300	200	0.60
UH	330	250	-	0.50
UH$^{\text{v}}$	330	[329, 250]	(0, 25,000]	0.50
UC	15	30	-	0.50
UC$^{\text{v}}$	15	[16, 30]	(0, 35,000]	0.50

HEX costs: $c_{\text{f}} = 2000$ \$/y, $c_{\text{v}} = 70$ \$/(m$^{2\beta}$ y), $\beta = 1$; Utility costs: $c_{\text{hu}} = 60$ \$/(kW y), $c_{\text{cu}} = 6$ \$/(kW y); Min. approach temperature: $\Delta T_{\text{min}} = 1$ °C.

Results

As can be seen from Table 5, the number of binary variables for the var UC and UH case has more than tripled compared to the base case. Due to the higher complexity, the computation time also increases from 133.95 s to 590.12 s.

Table 5. Problem size, computation time, and relative gap for CS2.

Case	Variables / -	Binaries / -	Time / s	Rel. Gap / %
base	1009	387	133.95	0.0096
var UC & UH	3014	1201	590.12	0.0000

Table 6 lists a comparison of the calculated values with data from the literature. Linnhoff and Ahmad [20] used the pinch design method and the driving force plot to obtain a HEN with 2.9300×10^6 \$/y of TAC. Through evolution and continuous optimization of the exchanger duties, they were able to obtain TAC of 2.8900×10^6 \$/y. In both calculations, the minimum temperature difference at the hot utility of 26 °C was violated, causing the outlet temperature of the thermal oil to be higher than 250 °C. Fieg et al. [21] corrected this by calculating the hot utility costs proportional to the thermal oil mass flow rate as a function of the outlet temperature. The TAC of 2.9300×10^6 \$/y was corrected to 2.9920×10^6 \$/y, and of 2.8900×10^6 \$/y to 3.0250×10^6 \$/y, respectively. Fieg et al. [21] also calculated an even cheaper solution with 2.9223×10^6 \$/y of TAC using a hybrid genetic algorithm (GA). Lewin [22] used a GA to find several solutions using different parameters of the algorithm. Despite an assumed minimum temperature difference of 10 °C, the outlet temperature of the hot utility was raised without considering mass-flow-dependent costs. The best solution has a TAC of 2.9360×10^6 \$/y. Zhu et al. [23] found the most expensive solution so far with TAC of 2.9700×10^6 \$/y through a two-step procedure using heuristics and nonlinear optimization. The optimizations performed in the literature enable a HEN with three stages and stream splits. In order to be able to compare our results

with the literature, we assume, on the one hand, that the costs are proportional to the heat flow. On the other hand, we use a lower bound for the minimum temperature difference of 1 °C.

For the base case, TAC of 2.9114×10^6 \$/y could be calculated using only two stages and stream splits. Compared to the best literature value from Linnhoff and Ahmad [20], this solution is 0.74% more expensive. Compared to the worst literature value from Zhu et al. [23], however, it is 2.01% cheaper.

Table 6. Results for CS2: Comparison of costs and heat loads at the utilities and streams.

Reference	TAC / 10^6 \$/y	Heat Load / MW		
		CU	HU	Stream
Linnhoff & Ahmad [20] [a]	2.9300	32.76	25.04	61.14
Linnhoff & Ahmad [20] [b]	2.8900	33.03	25.31	60.87
Zhu et al. [23]	2.9700	33.94	26.22	/[*]
Lewin [22]	2.9360	32.81	25.09	61.09
Fieg et al. [21]	2.9223	31.34	23.62	62.57
this work—base	2.9114	31.42	23.70	62.48
this work—var UC & UH	2.8526	31.43	23.71	62.47

[a] Figure 19 (a) of [20]. [b] Figure 19 (b) of [20]. [*] Heat load is not reported by the authors.

The TAC can be reduced to 2.8526×10^6 \$/y by implementing a CUS and a HUS. Compared to the best literature value provided by Linnhoff and Ahmad [20], the solution of the var UC and UH case is 1.30% cheaper. The heat loads differ only slightly in both cases. The stream plots are shown in Appendix B. The stream matches of the hot and cold streams are identical in both cases. The hot utility is used on the cold streams C1, C2, and C5 in both cases. The outlet temperature of the hot utility increases from 250.0 °C to 328.1 °C. The cold utility is used in the base case and the var UC and UH case on streams H1, H3, and H4. In the var UC and UH case, the cold utility is used a second time on stream H4. In this case, the CUS exchanges heat at two stages with the hot streams. The outlet temperature of the cooling water decreases from 30.0 °C to 16.8 °C. Analogous to CS1, based on the cost structure and its relative change to the base case costs in Figure 6, the most significant cost reduction can be found in the heat exchanger areas for hot and cold utilities.
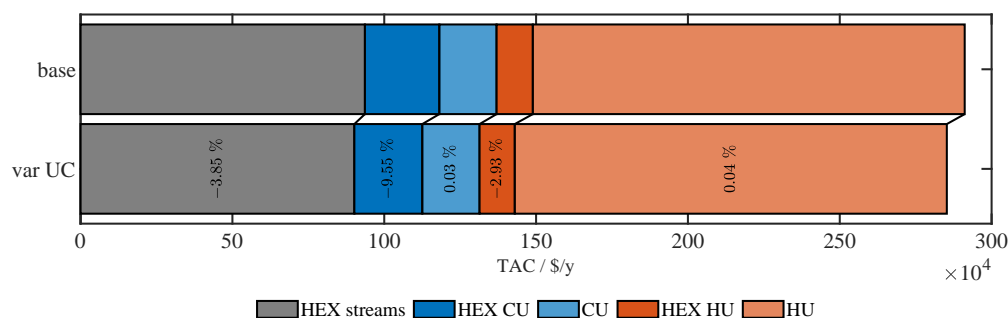

Figure 6. Breakdown of the cost structure for CS2. Relative cost savings in relation to the cost components of the base case.

3.4. Case Study 3

The third case study is the Bandar Imam aromatic plant on the northwestern coast of the Persian Gulf. The real-world problem includes six hot and ten cold streams. The stream data was provided by Khorasany and Fesanghary [19] and is listed in Table 7. Khorasany and Fesanghary [19] probably made a conversion error from °C to K for the cold utility [24–27]. Since cooling water is used as cold utility, it is implemented as CUS. In this case, two hot utilties are available: flue gas (UH_1) and steam (UH_2). The flue gas utility is implemented as HUS. The steam utility is implemented as a conventional utility without variable temperatures and flow capacity.

Table 7. Stream data for case study 3: Khorasany and Fesanghary [19].

Stream	T^{in} / °C	T^{out} / °C	F / kW/K	h / kW/m²/K
H1	385.0	159.0	131.51	1.238
H2	516.0	43.0	1198.96	0.546
H3	132.0	82.0	378.96	0.771
H4	91.0	60.0	589.55	0.859
H5	217.0	43.0	186.22	1.000
H6	649.0	43.0	116.00	1.000
C1	30.0	385.0	119.10	1.850
C2	99.0	471.0	191.05	1.129
C3	437.0	521.0	377.91	0.815
C4	78.0	418.6	160.43	1.000
C5	217.0	234.0	1297.70	0.443
C6	256.0	266.0	2753.00	2.085
C7	49.0	149.0	197.39	1.000
C8	59.0	163.4	123.56	1.063
C9	163.0	649.0	95.98	1.810
C10	219.0	221.3	1997.50	1.377
UH_1	1800.0	800.0	-	1.200
UH_1^v	1800.0	[800.0, 1700.0]	(0, 150.00]	1.200
UH_2	509.0	509.0	-	1.000
UC	38.0	82.0	-	1.000
UC^v	38.0	[39.0, 82.0]	[10,000, 500,000]	1.000

HEX costs: $c_f = 26\,600\,\$/\text{y}$, $c_v = 4147.5\,\$/(\text{m}^{2\beta}\,\text{y})$, $\beta = 0.6$; Hot utility costs: $c_{hu,1} = 35\,\$/(\text{kW}\,\text{y})$, $c_{hu,2} = 27\,\$/(\text{kW}\,\text{y})$; Cold utility costs: $c_{cu} = 2.1\,\$/(\text{kW}\,\text{y})$; Min. approach temperature: $\Delta T_{min} = 1\,°\text{C}$.

Results

Table 8 lists the number of variables, computation time, and relative gap. Both cases were optimally solved within the defined MIP gap. Due to the high complexity of the var UC and UH case, the computation time is the highest with 11,335.64 s (3.15 h).

Table 8. Problem size, computation time, and relative gap for CS3.

Case	Variables / -	Binaries / -	Time / s	Rel. Gap / %
base	2893	1128	637.07	0.0094
var UC & UH	7302	2914	11,335.64	0.0100

Table 9 compares the TAC and heat loads of the existing power plant with those from literature and those calculated in this paper. Khorasany and Fesanghary [19] used the same two-level approach as for CS1 to optimize the HEN of the aromatic plant. The optimized HEN with TAC of 7.4357×10^6 \$/y results in a cost savings of 16.00% compared to the existing plant. Feyli et al. [25] found TAC of 7.1285×10^6 \$/y using GA and a quasi-linear programming method. The HEN has eight stages and no stream splits. Aguitoni et al. [28] found a slight improvement in TAC. Here, the discrete variables were optimized with a GA and the heat loads on the streams, and the stream split fractions were optimized with the help of differential evolution. The resulting HEN has three stages with stream splits. Pavão et al. followed a two-level approach in [24,29], handling the binary variables with simulated annealing. The continuous variables are optimized using a rocket fireworks approach. In [29], the super-structure formulation was adapted, allowing intermediate placement of utilities. In [24], sub-stages, sub-splits, and cross-flows are additionally enabled. Nair and Karimi [26] used a stageless superstructure formulation with stream splits to optimize the TAC. Here, MILP relaxations are solved to find a lower bound on the TAC. Constraining the configurations and solving the nonlinear problem yield to an upper bound on the TAC. The lowest TAC to date of 6.6647×10^6 \$/y could be determined by Liu et al. [30] using a GA approach with intermediate utility placement.

In this paper, we obtained TAC of 6.7451×10^6 \$/y for the base case with two stages and stream splits. The stream plots are shown in Appendix B. Like most solutions from the literature, the second hot utility (steam) is not used. Compared to the best literature value of Liu et al. [30], this solution is 1.19% more expensive. However, our solution is 31.30% cheaper than the existing plant.

Table 9. Results for CS3: Comparison of costs and heat loads at the utilities and streams.

Reference	TAC / 10^6 \$/y	Heat Load / MW		
		CU	**HU**	**Stream**
existing plant [19]	8.8564	524.72	122.16	/*
Khorasany & Fesanghary [19]	7.4357	469.62	66.07	267.09
Feyli et al. [25]	7.1285	437.77	34.21	298.96
Aguitoni et al. [28]	7.1028	437.44	33.87	299.29
Pavão et al. [29]	6.8013	414.03	10.47	322.69
Pavão et al. [24]	6.7126	413.07	9.50	323.65
Nair & Karimi [26]	6.6956	412.25	8.69	324.47
Liu et al. [30]	6.6647	413.11	9.55	323.61
this work—base	6.7451	414.72	11.13	322.04
this work—var UC & UH	6.3297	416.57	12.98	320.18

/* Heat load is not reported by the authors.

In the var UC and UH case, the TAC can be reduced to 6.3297×10^6 \$/y through the implementation of a HUS and a CUS. Thus, this solution is 5.37% cheaper than the best solution provided by Liu et al. [30]. Compared to the existing plant, the TAC can be reduced by 40.49%. In the base and var UC and UH case, the second utility (steam) is not used. The HEN configuration of the two cases differs only in the first and fifth hot stream; see Appendix B. The outlet temperature of the first utility (flue gas) is increased from $800.0\,°C$ to $1674.4\,°C$. The outlet temperature of the cold utility is lowered from $82.0\,°C$ to $39.6\,°C$. Therefore, the LMTD at the HEX will be increased, resulting in smaller and more cost-efficient HEX areas. According to Figure 7, 16.55% and 11.00%, respectively, of the utility heat exchanger cost can be saved.
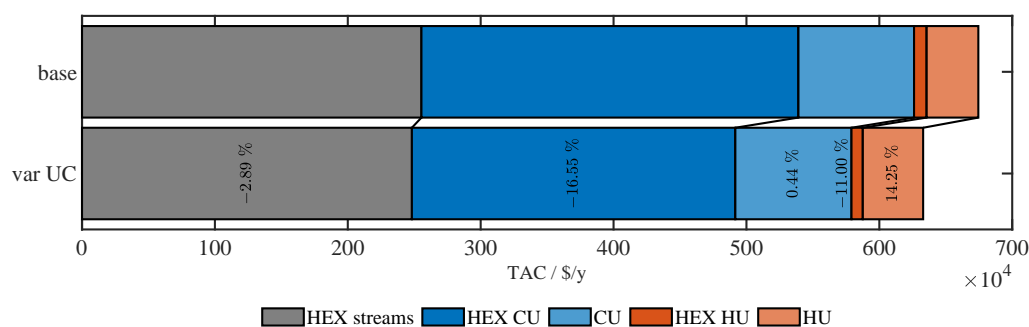

Figure 7. Breakdown of the cost structure for CS3. Relative cost savings in relation to the cost components of the base case.

4. Conclusions

We present an adapted superstructure formulation to consider streams with variable temperatures and flow capacities in the HEN design problem. We use piecewise-linear models with logarithmic coding to leverage the potential of state-of-the-art MILP solvers and to keep the problem traceable. The method is applied to represent utilities as streams. An essential novelty is that utility temperatures and flow capacities do not have to be defined a priori. Instead, only a technically viable range is defined. Further, compared to standard approaches, the utilities can exchange heat at multiple stages with stream splits and do not necessarily have to be placed at the stream ends. By coupling the design optimization of the HEN and the utilities, comprehensive results can be obtained.

By increasing the degree of freedom, the holistic process simulation provides the ability to find more efficient HENs and thus reduces costs and resources.

The method presented in this paper was applied to three representative case studies with 4, 9, and 16 streams, respectively. To verify the developed framework, a base case without utility streams was calculated and compared with results from the literature. Our results show only a minor deviation below 1.20% for all case studies, which indicates that our adapted superstructure formulation provides correct results within the expected error range resulting from the piecewise linear approximations and the MIP gap of the solver. To evaluate the potential of unchained HENS, we defined ranges for temperatures and flow capacities for the utilities and compared the results with respect to the base case. For CS1, a cost reduction of 0.29% can be achieved by implementing only the cold utility as a stream. For CS2 and CS3, both the hot and cold utilities were implemented as streams. Cost reductions of 1.30% and 5.37% were achieved, respectively. The results show that in a HEN with utility parameters defined in a specific range, the outlet temperature of cold utilities tends to the lower temperature limit. In contrast, the outlet temperature of hot utilities tends to the upper temperature limit. The resulting small temperature differences between inlet and outlet temperatures at the utilities result in a large LMTD at the heat exchangers. Therefore, the HEX areas can be reduced for the same amount of heat to be transferred, leading to lower TAC. In cases where, for example, the cost structure of the utilities does not depend linearly on the heat to be transferred or the mass flow is limited, a general prediction of the expected temperature is no longer feasible. With our method, these phenomena can be considered, and the coupled optimization of HEN and utilities will lead to cost-optimal results.

Our results of the three representative case studies demonstrate the relevance and versatility of our method. Using multi-stage utilities with stream splits, which do not necessarily have to be located at the stream ends, offers previously untapped potential for efficient utility placement. Loosening strictly defined stream parameters towards the definition of technically permissible ranges additionally generates new possibilities for coupled optimization of utilities and HEN. Moreover, the presented method serves as a foundation to couple the operational characteristics of stream parameter influencing systems into the HENS framework. This will create new opportunities to reduce costs and help to achieve urgently needed emission reduction through holistic process optimization.

Author Contributions: Conceptualization, D.H., F.B. and R.H.; methodology, D.H. and F.B.; formal analysis, D.H. and F.B.; writing—original draft preparation, D.H.; writing—review and editing, D.H., F.B. and R.H.; visualization, D.H.; supervision, F.B. and R.H.; funding acquisition, R.H. All authors have read and agreed to the published version of the manuscript.

Data Availability Statement: No new data were created or analyzed in this study. Data sharing is not applicable to this article.

Conflicts of Interest: The authors declare no conflict of interest.

Nomenclature

Acronyms
CS   case study
CUS   cold utility stream
GA   genetic algorithm
HEN   heat exchanger network
HENS   heat exchanger network synthesis
HEX   heat exchanger

HUS	hot utility stream	
MILP	mixed-integer linear programming	
PtL	Power-to-Liquid	
RMSE	root-mean-square error	
SSE	sum of squares error	
TAC	total annual cos	
US	utility stream	

Superscripts

in	inlet	
out	outlet	
v	variable utility paramters	

Subscripts

cu	cold utility	
hu	hot utility	
s	stream	
i	hot stream	
j	cold stream	
k	temperature stage	

Parameters

β	cost exponent	
ΔT_{min}	minimum approach temperature °C	
Γ	upper bound for temperature difference	°C
Ω	upper bound for heat exchange	kW
ω	lower bound for heat exchange	kW
c_f	step-fixed HEX cost coefficient	€/y
c_v	variable HEX cost coefficient	€/m$^{2\beta}$y
c_{cs}	cost coefficient for cold streams	€/kWy
c_{cu}	cost coefficient for cold utilities	€/kWy
c_{hs}	cost coefficient for hot streams	€/kWy
c_{hu}	cost coefficient for hot utilities	€/kWy
F	flow capacity	kW/K
h	heat transfer coefficient	kW/m^{2}K
n	dimension	
N_{cs}	number of cold streams	
N_{hs}	number of hot streams	
N_{st}	number of stages	
U	heat transfer coefficient for matches	kW/m^{2}K

Sets

$C_F = \{j \mid j$ is cold utility stream with variable flow capacity$\}$
$C_{Tin} = \{j \mid j$ is cold utility stream with variable inlet temperature$\}$
$C_{Tout} = \{j \mid j$ is cold utility stream with variable outlet temperature$\}$
$CP = \{j \mid j$ is cold process stream; $j = 1, \ldots, N_{cs}\}$
$H_F = \{i \mid i$ is hot utility stream with variable flow capacity$\}$
$H_{Tin} = \{i \mid i$ is hot utility stream with variable inlet temperature$\}$
$H_{Tout} = \{i \mid i$ is hot utility stream with variable outlet temperature$\}$
$HP = \{i \mid i$ is hot process stream; $i = 1, \ldots, N_{hs}\}$
$ST = \{k \mid k$ is temperature stage; $k = 1, \ldots, N_{st}\}$

Variables

ΔT	temperature difference	K
LMTD	logarithmic mean temperature difference	°C
TAC	total annual costs	€
F	flow capacity	kW/K
q	heat flow	kW
T	temperature	°C
z	binary variable for existance of HEX	

Appendix A. Convergence Behavior

The convergence behavior of the three case studies is based on the log-file of the solver and is shown in Figures A1–A3. The script to process the unformatted data into processable vectors was coded by ChatGPT [31].
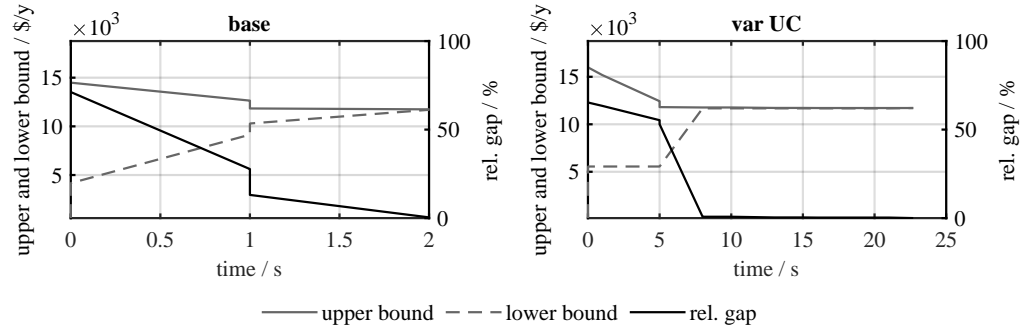

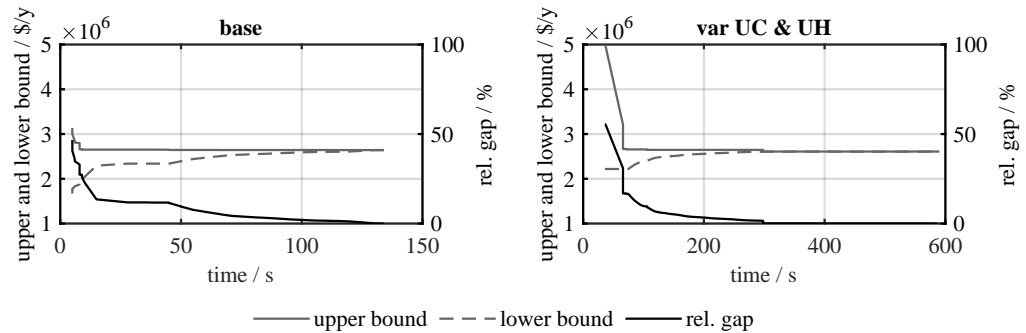**Figure A1.** Convergence behavior of CS1 for the base and the var UC case.

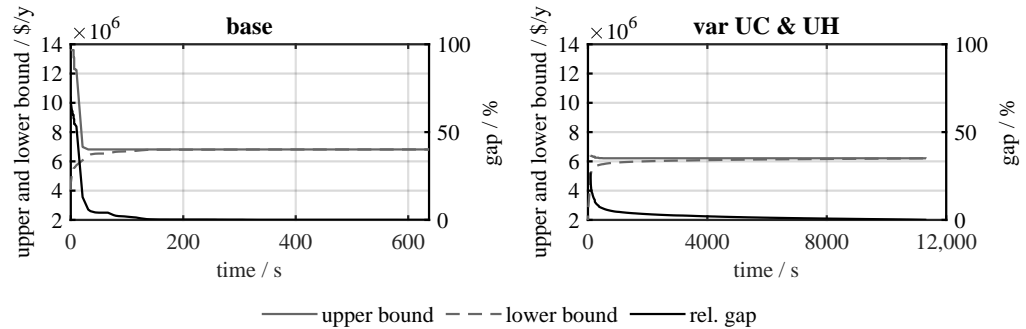**Figure A2.** Convergence behavior of CS2 for the base and the var UC and UH case.

Figure A3. Convergence behavior of CS3 for the base and the var UC and UH case.

Appendix B. Stream Plots

Figures A4–A9 show the optimized stream plots of the three case studies from Section 3. Hot streams are shown in red, and cold streams are shown in blue. The light gray circles inside the stages k represent heat exchangers. The dark gray circles without connecting lines are hot and cold utilities, respectively.
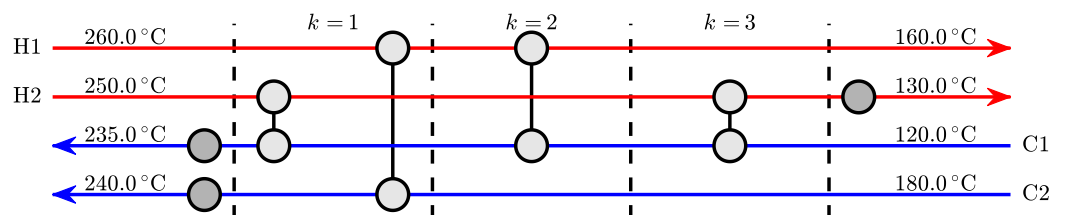
Figure A4. Optimized HEN configuration of CS1: base case with TAC of 1.1792×10^4 $/y.
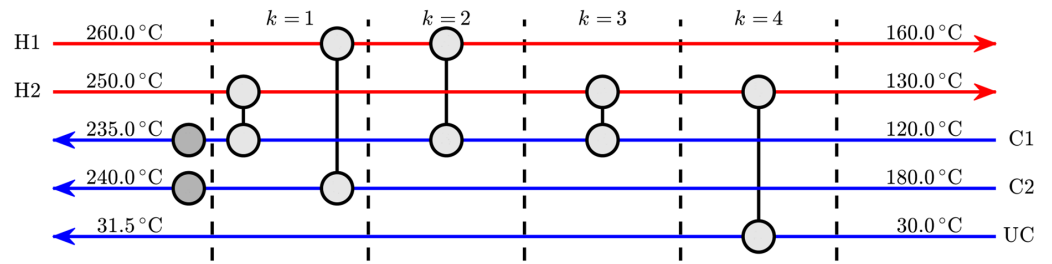
Figure A5. Optimized HEN configuration of CS1: var UC case with TAC of 1.1767×10^4 \$/y.
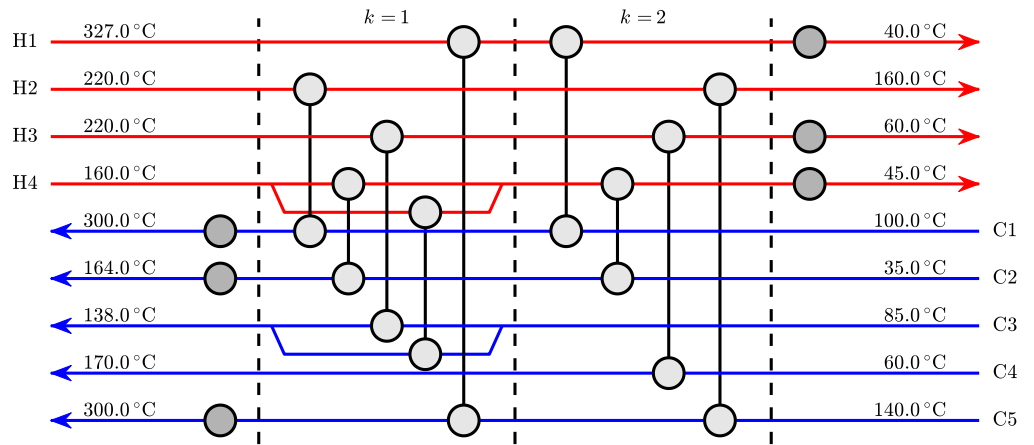
Figure A6. Optimized HEN configuration of CS2: base case with TAC of 2.9114×10^6 \$/y.
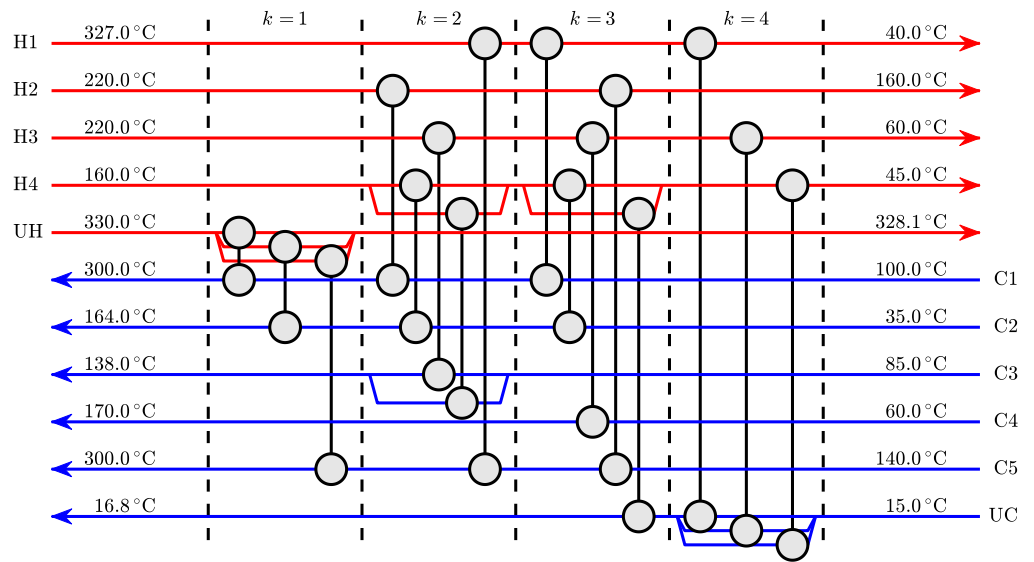
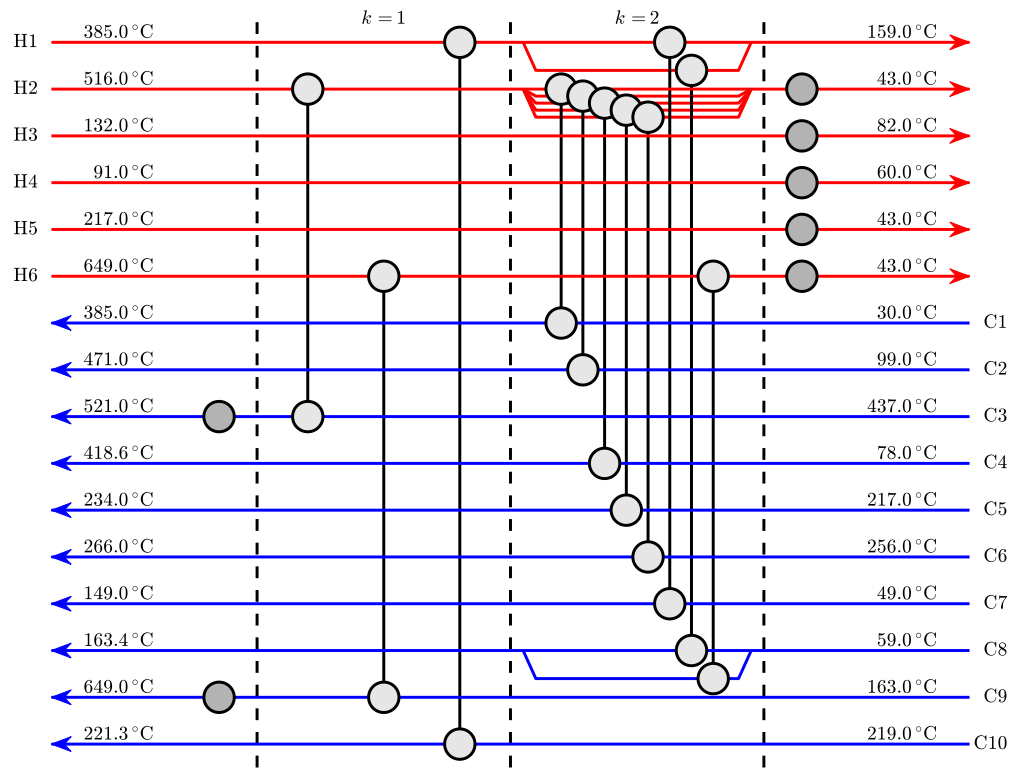**Figure A7.** Optimized HEN configuration of CS2: var UC & UH case with TAC of 2.8526×10^6 \$/y.

Figure A8. Optimized HEN configuration of CS3: base case with 6.7451×10^6 \$/y. Note that in this case only the flue gas is used as a hot utility.
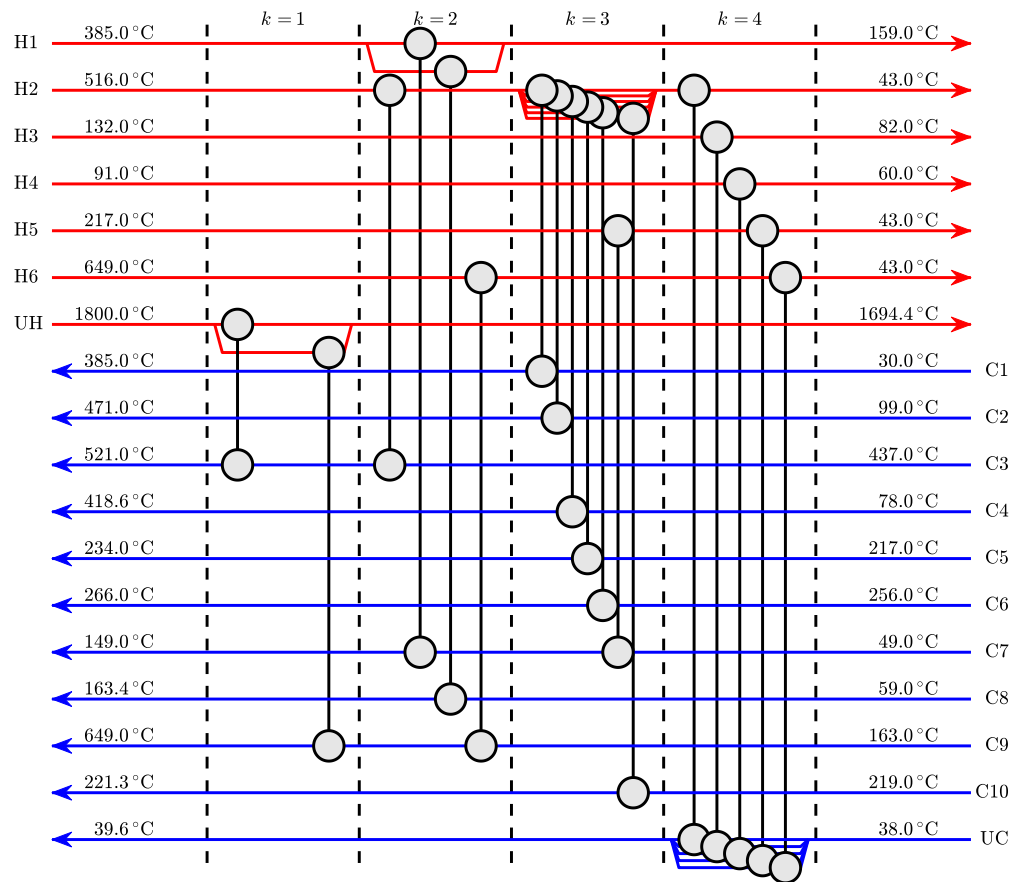

Figure A9. Optimized HEN configuration of CS3: var UC and UH case with TAC of 6.3297×10^6 \$/y. Note that in this case only the flue gas is used as a hot utility.

References

1.　Broeck, H.T. Economic Selection of Exchanger Sizes. *Ind. Eng. Chem.* **1944**, *36*, 64–67. [CrossRef]
2.　Masso, A.H.; Rudd, D.F. The synthesis of system designs. II. Heuristic structuring. *AIChE J.* **1969**, *15*, 10–17. [CrossRef]
3.　Ciric, A.R.; Floudas, C.A. Heat exchanger network synthesis without decomposition. *Comput. Chem. Eng.* **1991**, *15*, 385–396. [CrossRef]
4.　Yuan, X.; Pibouleau, L.; Domenech, S. Experiments in process synthesis via mixed-integer programming. *Chem. Eng. Process. Process Intensif.* **1989**, *25*, 99–116. [CrossRef]
5.　Yee, T.F.; Grossmann, I.E. Simultaneous optimization models for heat integration—II. Heat exchanger network synthesis. *Comput. Chem. Eng.* **1990**, *14*, 1165–1184. [CrossRef]
6.　Furman, K.C.; Sahinidis, N.V. A Critical Review and Annotated Bibliography for Heat Exchanger Network Synthesis in the 20th Century. *Ind. Eng. Chem. Res.* **2002**, *41*, 2335–2370. [CrossRef]
7.　Escobar, M.; Trierweiler, J.O. Optimal heat exchanger network synthesis: A case study comparison. *Appl. Therm. Eng.* **2013**, *51*, 801–826. [CrossRef]
8.　Gu, S.; Liu, L.; Zhang, L.; Bai, Y.; Wang, S.; Du, J. Heat exchanger network synthesis integrated with flexibility and controllability. *Chin. J. Chem. Eng.* **2019**, *27*, 1474–1484. [CrossRef]
9.　Zirngast, K.; Kravanja, Z.; Novak Pintarič, Z. An improved algorithm for synthesis of heat exchanger network with a large number of uncertain parameters. *Energy* **2021**, *233*, 121199. [CrossRef]
10.　Furman, K.C.; Sahinidis, N.V. Computational complexity of heat exchanger network synthesis. *Comput. Chem. Eng.* **2001**, *25*, 1371–1390. [CrossRef]
11.　Martelli, E.; Elsido, C.; Mian, A.; Marechal, F. MINLP model and two-stage algorithm for the simultaneous synthesis of heat exchanger networks, utility systems and heat recovery cycles. *Comput. Chem. Eng.* **2017**, *106*, 663–689. [CrossRef]
12.　Beck, A.; Hofmann, R. A Novel Approach for Linearization of a MINLP Stage-Wise Superstructure Formulation. *Comput. Chem. Eng.* **2018**, *112*, 17–26. [CrossRef]
13.　Vielma, J.P.; Nemhauser, G.L. Modeling disjunctive constraints with a logarithmic number of binary variables and constraints. *Math. Program.* **2011**, *128*, 49–72. [CrossRef]
14.　Camm, J.D.; Raturi, A.S.; Tsubakitani, S. Cutting Big M Down to Size. *Interfaces* **1990**, *20*, 61–66. [CrossRef]
15.　Löfberg, J. YALMIP: A toolbox for modeling and optimization in MATLAB. In Proceedings of the 2004 IEEE International Conference on Robotics and Automation (IEEE Cat. No.04CH37508), Taipei, Taiwan, 2–4 September 2004; pp. 284–289. [CrossRef]
16.　The MathWorks Inc. *MATLAB*, Version 9.13.0 (R2022b). 2022. Available online: https://de.mathworks.com/ (accessed on 8 December 2022).
17.　Ahmad, S. Heat Exchanger Networks: Cost Trade-Offs in Energy and Capital. Ph.D. Thesis, UMIST, Manchester, UK,1985.
18.　Nielsen, J.S.; Weel Hansen, M.; bay Joergensen, S. Heat exchanger network modelling framework for optimal design and retrofitting. *Comput. Chem. Eng.* **1996**, *20*, S249–S254. [CrossRef]
19.　Khorasany, R.M.; Fesanghary, M. A novel approach for synthesis of cost-optimal heat exchanger networks. *Comput. Chem. Eng.* **2009**, *33*, 1363–1370. [CrossRef]
20.　Linnhoff, B.; Ahmad, S. Cost optimum heat exchanger networks—1. Minimum energy and capital using simple models for capital cost. *Comput. Chem. Eng.* **1990**, *14*, 729–750. [CrossRef]
21.　Fieg, G.; Luo, X.; Jeżowski, J. A monogenetic algorithm for optimal design of large-scale heat exchanger networks. *Chem. Eng. Process. Process Intensif.* **2009**, *48*, 1506–1516. [CrossRef]
22.　Lewin, D.R. A generalized method for HEN synthesis using stochastic optimization — II. *Comput. Chem. Eng.* **1998**, *22*, 1387–1405. [CrossRef]
23.　Zhu, X.; O'Neil, B.; Roach, J.; Wood, R. A method for automated heat exchanger network synthesis using block decomposition and non-linear optimization. *Chem. Eng. Res. Des.* **1995**, *73*, 919–930.
24.　Pavão, L.V.; Costa, C.B.; Ravagnani, M.A. A new stage-wise superstructure for heat exchanger network synthesis considering substages, sub-splits and cross flows. *Appl. Therm. Eng.* **2018**, *143*, 719–735. [CrossRef]
25.　Feyli, B.; Soltani, H.; Hajimohammadi, R.; Fallahi-Samberan, M.; Eyvazzadeh, A. A reliable approach for heat exchanger networks synthesis with stream splitting by coupling genetic algorithm with modified quasi-linear programming method. *Chem. Eng. Sci.* **2022**, *248*, 117140. [CrossRef]
26.　Nair, S.K.; Karimi, I.A. Unified Heat Exchanger Network Synthesis via a Stageless Superstructure. *Ind. Eng. Chem. Res.* **2019**, *58*, 5984–6001. [CrossRef]
27.　Kayange, H.A.; Cui, G.; Xu, Y.; Li, J.; Xiao, Y. Non-structural model for heat exchanger network synthesis allowing for stream splitting. *Energy* **2020**, *201*, 117461. [CrossRef]
28.　Aguitoni, M.C.; Pavão, L.V.; Siqueira, P.H.; Jiménez, L.; Ravagnani, M.A.d.S.S. Heat exchanger network synthesis using genetic algorithm and differential evolution. *Comput. Chem. Eng.* **2018**, *117*, 82–96. [CrossRef]
29.　Pavão, L.V.; Costa, C.B.B.; Ravagnani, M.A.S.S. An Enhanced Stage-wise Superstructure for Heat Exchanger Networks Synthesis with New Options for Heaters and Coolers Placement. *Ind. Eng. Chem. Res.* **2018**, *57*, 2560–2573. [CrossRef]

30. Liu, Z.; Yang, L.; Yang, S.; Qian, Y. An extended stage-wise superstructure for heat exchanger network synthesis with intermediate placement of multiple utilities. *Energy* **2022**, *248*, 123372. [CrossRef]
31. OpenAI. Assistant. 2022. Available online: https://chat.openai.com/ (accessed on 21 December 2022).